Dynamical thermal conductivity of bulk semiconductor crystals

Younes Ezzahri, Karl Joulain

Dynamical thermal conductivity of bulk semiconductor crystals

Younès Ezzahri and Karl Joulain

Citation: Journal of Applied Physics **112**, 083515 (2012); doi: 10.1063/1.4759366
View online: http://dx.doi.org/10.1063/1.4759366
View Table of Contents: http://scitation.aip.org/content/aip/journal/jap/112/8?ver=pdfcov
Published by the AIP Publishing

Dynamical thermal conductivity of bulk semiconductor crystals

Younès Ezzahri[a] and Karl Joulain
Institut Pprime, CNRS-Université de Poitiers-ENSMA, Département Fluides, Thermique, Combustion, ENSIP-Bâtiment de mécanique, 2 rue Pierre Brousse, F 86022 Poitiers, Cedex, France

(Received 30 May 2012; accepted 25 September 2012; published online 22 October 2012)

The paper discusses the behavior of the dynamical lattice thermal conductivity $\kappa(\Omega)$ of bulk semiconductor crystals. The calculation approach is based on solving Boltzmann-Peierls phonon transport equation in the frequency domain after excitation by a dynamical temperature gradient, within the framework of the single relaxation time approximation and using modified Debye-Callaway model. Our model allows us to obtain a compact expression for $\kappa(\Omega)$ that captures the leading behavior of the dynamical thermal conduction by phonons. This expression fulfils the causality requirement and leads to a convolution type relationship between the heat flux density current and the temperature gradient in the real space-time domain in agreement with Gurtin-Pipkin theory. The dynamical behavior of $\kappa(\Omega)$ is studied by changing temperature as well as different intrinsic and extrinsic parameters. Our calculations show the cut-off frequency of $\kappa(\Omega)$ to be sensitive to the changes of some of these parameters. The paper investigates also the applicability of Shastry's sum rule (SSR) in the frame work of Boltzmann theory. It is shown that within the frame work of Callaway approximated form of the collision operator and time independent Callaway parameter, the SSR breaks down and is only valid when resistive processes dominate normal processes, for which case, we derive an alternative expression to the classical limit of the expectation of the thermal operator introduced in Shastry's formalism. © *2012 American Institute of Physics*. [http://dx.doi.org/10.1063/1.4759366]

I. INTRODUCTION

The thermal conductivity κ of bulk dielectric and semiconductor (SC) crystals in which energy (heat) is mainly carried by phonons, has been the object of many theoretical and experimental studies.[1–18] The steady-state behavior of which has been understood for many decades. According to the pioneer work of Debye and Peierls[1] and many experimental works later,[12–14,17,18] κ has a universal behavior as a function of temperature: κ depends on the size and shape of the crystal at low temperatures where the mean free path (MFP) of the phonon becomes of the order of the dimensions of the crystal. At this temperature regime, κ mirrors the temperature behavior of the specific heat. κ increases with temperature and reaches a maximum at about $T \approx 0.05\theta_D$, where θ_D is an average Debye temperature over all phonon polarization branches of the crystal. Above this maximum κ is limited by scattering of phonons amongst themselves via anharmonic scattering processes, more essentially Umklapp processes (U-processes) and is characteristic of the material crystal. The effect of impurities or imperfections in the crystal to scatter phonons is particularly important near the maximum where both boundary scattering and anharmonic scattering processes are present but weak.

At short time scales, a number of unfamiliar and intriguing phenomena have been predicted and few of them have been observed. Energy transport at very short time scales where local nonequilibrium regime appears is probably the most interesting one.[19,20] The question of energy and heat transport mechanisms at short time and length scales is the basis of numerous theoretical and experimental papers.[19–27] The study of energy and heat transport at very short time scales has even become crucial and more needed recently due to the continuous increasing of clock speeds and decreasing of feature sizes in microelectronic and optoelectronic applications.[28] Clock speeds of present microprocessors based on silicon technology are of few gigahertz, and according to the International Technology Roadmap for Semiconductors (ITRS), devices with clock speeds of few tens of gigahertz will be available in the next decade.[28]

In the past, only few works addressed the question of studying the time and dynamical behaviors of the thermal conductivity of SC crystals. Most of the works were theoretical; the most cited ones are Guyer and Krumhansl,[29–31] Volz,[32,33] Alvarez and Jou,[25,26] Hüttner,[34] and Shastry.[35,36] Based on these works, the expected cut-off frequency f_C of the dynamical thermal conductivity has usually been theorized to be on the order of $f_C > 1/\tau$ where τ is the relaxation time of the dominant phonons during the heat transport phenomenon. Volz[33] showed that the thermal conductivity κ of Si decreases at frequencies $f\tau > 1$. The life time at room temperature of dominant phonons in SC alloys is ~100 ps, and then the expected f_C based on the former theoretical investigation is $f_C > 10$ GHz. For his prediction, Volz[32,33] used two different methods, (1) molecular dynamics and (2) the expression of κ based on Boltzmann-Peierls equation in the grey spectrum approximation (GSA) (constant relaxation time). A constant relaxation time, however, seems to be a very poor approximation, especially when considering the dynamical behavior of energy transport. At the top of this short list of theoretical works, is the remarkable and interesting work of Shastry,[35,36]

[a]Author to whom correspondence should be addressed. Electronic mail: younes.ezzahri@univ-poitiers.fr.

in which he introduced a new formalism to study the dynamical behavior of not only thermal conductivity but also other thermoelectric properties (electrical conductivity, Seebeck coefficient, and Lorentz number) for different condensed matter models. Even though Shastry did not discuss the behavior of the cut-off frequency of the dynamical thermal conductivity, he introduced a new sum rule of the real part of the latter, in analogy to the well established *f*-sum rule of the real part of the electrical conductivity.[36]

Recently, Koh and Cahill reported the most notable and cited experimental work so far regarding the frequency behavior of the thermal conductivity of SC crystal alloys.[37] Using time domain thermoreflectance (TDTR),[38–40] the authors measured the thermal conductivity of a number of SC crystals including alloys and single crystals as a function of the frequency of excitation of the heat source which, in the experiment was the modulation frequency of the laser pump beam.[38–40] The analysis of the dynamical behavior of the thermal conductivity at room temperature showed a cut-off frequency f_C smaller than 10 MHz for SC alloys. On the other hand, the thermal conductivity of single SC crystals showed a plateau over the whole range of frequency used in the experiment (0.6–10 MHz).[37] This surprising result came to defy all previous theoretical investigations of the frequency or time dependence of the thermal conductivity of SC crystals.

To explain their valuable observations, Koh and Cahill[37] made the statement that all phonons with MFP longer than the thermal penetration depth $\delta(\Omega)$, where Ω is the circular frequency of the excitation source, transport heat ballistically and as such would not contribute to the thermal conductivity $\kappa(\Omega)$ measured in the TDTR experiment, we will refer to this statement later in the discussion section as *Koh and Cahill statement*. Using a modified Debye-Callaway formalism as first proposed by Asen-Palmer *et al.*[17] and Morelli *et al.*,[18] the authors translate their assumption as a boundary scattering process that phonons would undergo at a virtual interface. This virtual interface is actually the surface of a sphere whose radius is the thermal penetration depth $\delta(\Omega)$. The authors found a satisfactory agreement between experimental data and the results of this phenomenological approach. We will get back to comment on this at the end of the discussion section.

The motivation behind the current work is twofold. First, we present an approach within the frame work of Boltzmann kinetic theory of phonon transport using the Callaway approximation of the collision operator in order to calculate and develop a compact formula capturing the leading dynamical behavior of the lattice thermal conductivity of bulk SC crystals $\kappa(\Omega)$, which will shed more light on the effect of different intrinsic and extrinsic parameters in influencing this dynamics. Second, we investigate the conditions under which Shastry's sum rule (SSR) holds in the frame work of Boltzmann theory and we give an alternative expression to the classical limit of the expectation of the thermal operator introduced in Shastry's formalism.[35,36]

The detail of the theoretical derivation of $\kappa(\Omega)$ is presented in the next section. In the third section, we discuss the results of this approach by analyzing the effect of varying different intrinsic and extrinsic parameters of bulk SC crystals. At the end of this section, we comment on the recent experimental data of Koh and Cahill,[37] then we discuss the applicability of Shastry's sum rule and we finish with a summary and concluding remarks.

II. THEORY

Our goal in this section is to develop a compact expression of the dynamical lattice thermal conductivity $\kappa(\Omega)$ of bulk SC crystals that gives an insight onto the leading behavior in their response to a dynamical temperature gradient. The latter could originate from application of a periodic heat source at the surface of the SC crystal, as was the case in the experimental work of Koh and Cahill,[37] or within its volume.

A. Boltzmann-Peierls transport equation (BPTE)

To develop an expression for $\kappa(\Omega)$ of a bulk SC crystal, one starts with BPTE. As many of the previous investigations,[1–18] the solution of this integral-differential equation is approximated by the use of the relaxation time concept in which the phonon scattering process is expressed in terms of the single relaxation time $\tau(\boldsymbol{q}, S)$ for a phonon of wave vector $\boldsymbol{q}$ and polarization S. In this case, the scattering cross sections are calculated using perturbation techniques.[1–4,6] In such an approach, the temperature and intrinsic frequency dependences of anharmonic three-phonon relaxation times are strongly dependent on the actual phonon polarization branch and on the dispersion relation of the phonon spectrum. The expressions derived for the relaxation times are only valid for specific phonons in a limited temperature range. For simplification, however, we assume the latter expressions to be valid for any temperature and we further assume an isotropic linear (Debye-like) phonon spectrum for each phonon polarization branch.

Callaway[5] approximation of the collision operator in BPTE allows a simple separation of normal processes (N-processes) and U-processes. The pioneer purely intuitive work of Callaway[5] was investigated in detail by many authors and more robust theoretical foundations have been found.[10,15,16] For their algebraically convenient forms, the Callaway[5] and Holland[11] methods have been the most and widely used formulations for the steady-state thermal conductivity $\kappa(T)$ that enable fitting of the experimental data for a large number of materials in which heat is carried by phonons, with only few number of adjustable parameters.

To derive $\kappa(\Omega)$, we extend the use to a broader time dependent phenomena of the same approach used by Asen-Palmer *et al.*[17] and later Morelli *et al.*,[18] and we make use of the modified Debye-Callaway model to explicitly include both longitudinal and transverse phonon modes. Although this model might be not very rigorous, the treatment is to some extent justified by the reasonable agreement with experiment that has been obtained with it in the steady-state.[17,18] In this approach, the contributions of longitudinal and transverse acoustic branches are considered separately, furthermore, any conversion of normal modes between both branches (inter-transitions) is neglected; only transitions within the same acoustic

branch (intra-transitions) are considered. This approach was first used by Holland[11] in his extension of Callaway model.[5]

We assume application of a temperature gradient along a direction $\vec{\imath}$, where $\vec{\imath}$ is a unit vector along a geometrical direction within the bulk SC crystal, this could be a principal crystal axis. Under the relaxation time approximation, the Callaway form of the BPTE for a phonon distribution function $n_S(x,\boldsymbol{q},t) \equiv n_{\boldsymbol{q},S}$ is given by

$$\frac{\partial \boldsymbol{n}_{\boldsymbol{q},S}}{\partial t} + \boldsymbol{V}_{\boldsymbol{q},S}.\nabla n_{\boldsymbol{q},S} = -\left.\frac{\partial n_{\boldsymbol{q},S}}{\partial t}\right|_{Coll} = \frac{n_{\boldsymbol{q},S}^{\boldsymbol{\lambda}_S} - n_{\boldsymbol{q},S}}{\tau_{\boldsymbol{q},S}^{N}} + \frac{n_{\boldsymbol{q},S}^{0} - n_{\boldsymbol{q},S}}{\tau_{\boldsymbol{q},S}^{R}}, \tag{1}$$

where $n_{\boldsymbol{q},S}^{0} = \left(e^{\frac{\hbar\omega_S(q)}{k_B T}} - 1\right)^{-1}$ is the equilibrium phonon Planck distribution function to which resistive phonon scattering processes (all scattering processes that change the total phonon wave vector: Umklapp, boundary, defects, imperfections) tend to return the phonon system with a single relaxation time $\tau_R(\boldsymbol{q},S)$. $\omega_S(\boldsymbol{q})$ is the dispersion relation of the phonon in state ($\boldsymbol{q}$, S), k_B and T are the Boltzmann constant and the absolute local temperature, respectively. On the other hand, the distribution function which is stationary for N-processes (scattering processes that do not change the total phonon wave vector) is not $n_{\boldsymbol{q},S}^{0}$ but rather $n_{\boldsymbol{q},S}^{\boldsymbol{\lambda}_S}$. N-processes lead the phonon system to a displaced (*drifted*) Planck distribution function $n_{\boldsymbol{q},S}^{\boldsymbol{\lambda}_S}$ with a single relaxation time $\tau_N(\boldsymbol{q},S)$, where $\boldsymbol{\lambda}_S$ is a vector that has the dimension of a velocity times Planck constant $\hbar$:[5,8]

$$n_{\boldsymbol{q},S}^{\boldsymbol{\lambda}_S} = \left[\exp\left(\frac{\hbar\omega_S(\boldsymbol{q}) - \boldsymbol{\lambda}_S.\boldsymbol{q}}{k_B T}\right) - 1\right]^{-1}. \tag{2}$$

$\boldsymbol{\lambda}_S/\hbar$ is called the drift velocity vector of the phonon ($\boldsymbol{q}$, S), while $\boldsymbol{V}_{\boldsymbol{q},S} = v_{S,\imath}\boldsymbol{q}_\imath = \partial\omega_S(\boldsymbol{q})/\partial\boldsymbol{q}_\imath$ is its group velocity vector, which in general depends on the direction of $\boldsymbol{q}_\imath$. Here, we assume the heat transport to be in the same direction as the applied temperature gradient.

In this analysis, we assume all relaxation times describing the different intrinsic and extrinsic phonon scattering processes, to be independent of the time or frequency dependence of the applied temperature gradient.

As in Callaway analysis,[5,8] the vector $\boldsymbol{\lambda}_S$ is assumed to have a very small module. Then, to first order in $\boldsymbol{\lambda}_S$, the Taylor's series expansion of $n_{\boldsymbol{q},S}^{\boldsymbol{\lambda}_S}$ such that $O(\boldsymbol{\lambda}_S^2)$ is neglected, gives

$$\begin{aligned} n_{\boldsymbol{q},S}^{\boldsymbol{\lambda}_S} &\equiv n_{\boldsymbol{q},S}(\boldsymbol{\lambda}_S) \cong n_{\boldsymbol{q},S}(0) + \boldsymbol{\lambda}_S.\left(\frac{\partial n_{\boldsymbol{q},S}(\boldsymbol{\lambda}_S)}{\partial \boldsymbol{\lambda}_S}\right)_{\boldsymbol{\lambda}_S=0} \\ &\cong n_{\boldsymbol{q},S}^{0} + \frac{\boldsymbol{\lambda}_S.\boldsymbol{q}}{k_B T}\frac{e^{\frac{\hbar\omega_{\boldsymbol{q},S}}{k_B T}}}{\left(e^{\frac{\hbar\omega_{\boldsymbol{q},S}}{k_B T}} - 1\right)^2} = n_{\boldsymbol{q},S}^{0} + \frac{(\boldsymbol{\lambda}_S.\boldsymbol{q})T}{\hbar\omega_{\boldsymbol{q},S}}\frac{dn_{\boldsymbol{q},S}^{0}}{dT}. \end{aligned} \tag{3}$$

In our analysis, we treat the bulk SC crystal as a continuum elastic isotropic linear medium, in which case and by symmetry consideration; $\boldsymbol{\lambda}_S$ must be a constant vector in the direction of the applied temperature gradient, so it is convenient to define still another parameter (Callaway parameter) β_S that has the dimension of a relaxation time:[5,8]

$$\boldsymbol{\lambda}_S = -\hbar\beta_S v_{S,\imath}^2\left(\frac{\nabla T}{T}\right). \tag{4}$$

Since we are dealing with Debye-like phonon dispersion relation $\omega_S(\boldsymbol{q}) \equiv \omega_{\boldsymbol{q},S} = v_{S,\imath}|\boldsymbol{q}|$, so that one considers heat transport due only to acoustic phonons, we have $\boldsymbol{q} = \frac{\boldsymbol{V}_{\boldsymbol{q},S}\omega_{\boldsymbol{q},S}}{v_{S,\imath}^2}$. This implies

$$\boldsymbol{\lambda}_S.\boldsymbol{q} = -\hbar\omega_{\boldsymbol{q},S}\beta_S\boldsymbol{V}_{\boldsymbol{q},S}.\left[\frac{\nabla T}{T}\right]. \tag{5}$$

To solve Eq. (1), we continue to use two more approximations that are usually made in the treatment of the steady-state case of BPTE; (1) The distribution function $n_{\boldsymbol{q},S}$ depends on the position only through the temperature $T(x)$:$\nabla n_{\boldsymbol{q},S} = \frac{dn_{\boldsymbol{q},S}}{dT}\nabla T$ and (2) it is assumed that deviation from equilibrium is small, i.e., $\frac{d\boldsymbol{n}_{\boldsymbol{q},S}}{dT} \cong \frac{dn_{\boldsymbol{q},S}^{0}}{dT_0}$, where T_0 is the absolute local equilibrium temperature.

When the expression $\boldsymbol{\lambda}_S.\boldsymbol{q}$ is substituted into Eq. (3) then in Eq. (1), and based on the above two approximations, Eq. (1) takes the form

$$\begin{aligned} &\frac{\partial n_{\boldsymbol{q},S}}{\partial t} + \boldsymbol{V}_{\boldsymbol{q},S}.\frac{dn_{\boldsymbol{q},S}^{0}}{dT_0}\nabla T = \frac{n_{\boldsymbol{q},S}^{0} - \boldsymbol{n}_{\boldsymbol{q},S}}{\tau_{\boldsymbol{q},S}^{C}} - \frac{\beta_S}{\tau_{\boldsymbol{q},S}^{N}}V_{\boldsymbol{q},S}.\frac{dn_{\boldsymbol{q},S}^{0}}{dT_0}\nabla T \\ &\Rightarrow \tau_{\boldsymbol{q},S}^{C}\frac{\partial \boldsymbol{n}_{\boldsymbol{q},S}}{\partial t} + \boldsymbol{n}_{\boldsymbol{q},S} = n_{\boldsymbol{q},S}^{0} - \tau_{\boldsymbol{q},S}^{C}\left[1 + \frac{\beta_S}{\tau_{\boldsymbol{q},S}^{N}}\right]\boldsymbol{V}_{\boldsymbol{q},S}.\frac{dn_{\boldsymbol{q},S}^{0}}{dT_0}\nabla T \\ &= n_{\boldsymbol{q},S}^{0} - \tau_{\boldsymbol{q},S}^{eff}\boldsymbol{V}_{\boldsymbol{q},S}.\frac{dn_{\boldsymbol{q},S}^{0}}{dT_0}\nabla T, \end{aligned} \tag{6}$$

where $\tau_{\boldsymbol{q},S}^{C}$ and $\tau_{\boldsymbol{q},S}^{eff}$ are, respectively, the "*combined*" and the "*effective total*" relaxation times given, respectively, by

$$\frac{1}{\tau_{\boldsymbol{q},S}^{C}} = \frac{1}{\tau_{\boldsymbol{q},S}^{N}} + \frac{1}{\tau_{\boldsymbol{q},S}^{R}} \quad \text{and} \quad \tau_{\boldsymbol{q},S}^{eff} = \tau_{\boldsymbol{q},S}^{C}\left[1 + \frac{\beta_S}{\tau_{\boldsymbol{q},S}^{N}}\right]. \tag{7}$$

In Eq. (6), the effect of N-processes is contained in the effective total relaxation time $\tau_{\boldsymbol{q},S}^{eff}$ which is a complicated quantity, depending on $\tau_{\boldsymbol{q},S}^{N}$, $\tau_{\boldsymbol{q},S}^{R}$, and β_S. This complication is necessary because of the behavior of N-processes which shuffle crystal momentum back and forth between normal modes, and then contribute implicitly to the thermal conductivity of a given SC crystal.[5,8]

As for all relaxation times considered in this study, and taking into account the approximations made above, we further assume that Callaway pseudo-relaxation time β_S is a constant independent of the time or frequency dependence of the applied temperature gradient, and thereby can be calculated similarly to the steady-state case.[5,8] This means that the dependence of the phonon gas drift on time and space is contained in the expression of the drift velocity $\boldsymbol{\lambda}_S/\hbar$ only through the applied dynamical temperature gradient $\nabla T(x,t)$.

For each acoustic phonon polarization branch, Callaway pseudo-relaxation time β_S is determined by recalling that N-processes cannot change the total phonon wave vector (total crystal momentum). In the steady-state case $(\partial n_{q,S}/\partial t = 0)$, β_S can be calculated following the same procedure of calculation as first performed by Callaway[5] and Carruthers.[8]

B. Dynamical thermal conductivity

In order to solve Eq. (6), we apply Fourier transform with respect to time to both sides. One obtains

$$(1 - j\Omega\tau^C_{q,S})\overline{n_{q,S}} = \overline{n^0_{q,S}} - \tau^{eff}_{q,S}\boldsymbol{V}_{q,S}.\frac{dn^0_{q,S}}{dT_0}\overline{\nabla T}$$

$$\Rightarrow \overline{n_{q,S}}(x,\Omega) = \frac{1}{1 - j\Omega\tau^C_{q,S}}\overline{n^0_{q,S}} - \frac{\tau^{eff}_{q,S}\boldsymbol{V}_{q,S}.\dfrac{dn^0_{q,S}}{dT_0}}{1 - j\Omega\tau^C_{q,S}}\overline{\nabla T}(x,\Omega), \tag{8}$$

where the top bars over $n_{q,S}$, $n^0_{q,S}$ and ∇T indicate Fourier transforms and j is the complex operator $(j^2 = -1)$.

Once we know the distribution function in Fourier (frequency) domain, the next step is the calculation of the heat flux density current $\overline{\boldsymbol{J}_Q}$ in the same domain along the direction of the applied temperature gradient. $\overline{\boldsymbol{J}_Q}$ is defined as

$$\overline{\boldsymbol{J}_Q}(x,\Omega) = \frac{1}{W}\sum_{q,S}\hbar\omega_S(\boldsymbol{q})\overline{n_{q,S}}(x,\Omega)\boldsymbol{V}_{q,S}$$

$$= -\frac{1}{W}\sum_{q,S}\hbar\omega_{q,S}v^2_{S,t}\frac{\tau^{eff}_{q,S}\frac{dn^0_{q,S}}{dT_0}}{1 - j\Omega\tau^C_{q,S}}\overline{\nabla T}(x,\Omega), \tag{9}$$

where we use W to denote the volume of the bulk SC crystal. We should note here that the contribution of the first term in Eq. (8) to $\overline{\boldsymbol{J}_Q}$ vanishes since the phonon equilibrium distribution $n^0_{q,S}$ can give no contribution to any energy (heat) transport.[1,6,8,16] The latter is an isotropic function in the wave vector $\boldsymbol{q}$ space while the velocity $\boldsymbol{V}_q$ is an algebraic function; the dispersion relation and the relaxation times depend on the module of the wave vector $\boldsymbol{q}$ and as such are even functions of q.

The density of states in the $\boldsymbol{q}$ space is very great; we can use the standard relation to replace the sum sign by an integral sign $(\sum_{q,S} \to \frac{W}{8\pi^3}\sum_S\int d^3\boldsymbol{q})$

$$\overline{\boldsymbol{J}_Q}(x,\Omega) = -\left[\frac{1}{8\pi^3}\sum_S\int\frac{\tau^{eff}_{q,S}}{1 - j\Omega\tau^C_{q,S}}v^2_{S,t}C_{Ph}(\boldsymbol{q},S)d^3\boldsymbol{q}\right]\overline{\nabla T}(x,\Omega)$$
$$= -\kappa(\Omega)\overline{\nabla T}(x,\Omega). \tag{10}$$

In Eq. (10), C_{Ph} represents the phonon specific heat or heat capacity per normal mode $C_{Ph}(\boldsymbol{q},S) = C_{Ph}(\omega_{q,S},T_0) = \hbar\omega_{q,S}dn^0_{q,S}/dT_0$.

By considering the dynamical temperature gradient and the heat flux density current Fourier-analyzed as in the customary way, we recognize from Eq. (10) the dynamical thermal conductivity $\kappa(\Omega)$ which takes the expression

$$\kappa(\Omega) = \frac{1}{8\pi^3}\sum_S\int\frac{\tau^{eff}_{q,S}}{1 - j\Omega\tau^C_{q,S}}v^2_{S,t}C_{Ph}(\boldsymbol{q},S)d^3\boldsymbol{q}. \tag{11}$$

Note that Ω represents the circular frequency which is related to the real frequency f by the standard definition $\Omega = 2\pi f$.

For simplification and further discussion (see Sec. III), we set

$$\kappa^0_{q,S} = \frac{1}{8\pi^3}\tau^{eff}_{q,S}v^2_{S,t}C_{Ph}(\boldsymbol{q},S) \tag{12}$$

$\kappa(\Omega)$ takes then the more compact form

$$\kappa(\Omega) = \sum_S\int\frac{\kappa^0_{q,S}}{1 - j\Omega\tau^C_{q,S}}d^3\boldsymbol{q} = \kappa_r(\Omega) + j\kappa_i(\Omega), \tag{13}$$

where κ_r and κ_i are, respectively, the real and the imaginary parts of $\kappa(\Omega)$

$$\begin{cases}\kappa_r(\Omega) = \sum_S\int\dfrac{\kappa^0_{q,S}}{1 + (\Omega\tau^C_{q,S})^2}d^3\boldsymbol{q}\\ \kappa_i(\Omega) = \sum_S\int\kappa^0_{q,S}\dfrac{\Omega\tau^C_{q,S}}{1 + (\Omega\tau^C_{q,S})^2}d^3\boldsymbol{q}.\end{cases} \tag{14}$$

To simplify more the expression of $\kappa(\Omega)$, we express it, as it is customary in the modified Debye-Callaway model, as the sum over one longitudinal (κ_L) and two degenerate transverse (κ_T) phonon polarization branches[18]

$$\kappa(\Omega) = \kappa_L(\Omega) + 2\kappa_T(\Omega). \tag{15}$$

By using the isotropy of the group velocity in the real and reciprocal spaces $v^2_{S,q_x} = v^2_{S,q_y} = v^2_{S,q_z} = \frac{1}{3}v^2_S$ and the usual change of variable $x = \hbar\omega/k_BT_0$, it is straightforward to show that the real part $\kappa_r(\Omega)$ takes the form

$$\begin{cases}\kappa_r(\Omega) = \kappa^r_L(\Omega) + 2\kappa^r_T(\Omega)\\ \kappa^r_S(\Omega) = \kappa^r_{S1}(\Omega) + \kappa^r_{S2}(\Omega)\\ \kappa^r_{S1}(\Omega) = \dfrac{1}{3}C_ST_0^3\displaystyle\int_0^{\theta^S_D/T_0}\frac{\tau^C_S(x)}{1 + [\Omega\tau^C_S(x)]^2}D(x)dx\\ \kappa^r_{S2}(\Omega) = \dfrac{1}{3}C_ST_0^3\beta_S\displaystyle\int_0^{\theta^S_D/T_0}\frac{\frac{\tau^C_S(x)}{\tau^N_S(x)}}{1 + [\Omega\tau^C_S(x)]^2}D(x)dx\end{cases} \tag{16}$$

and similarly for the imaginary part $\kappa_i(\Omega)$

$$\begin{cases}\kappa_i(\Omega) = \kappa^i_L(\Omega) + 2\kappa^i_T(\Omega)\\ \kappa^i_S(\Omega) = \kappa^i_{S1}(\Omega) + \kappa^i_{S2}(\Omega)\\ \kappa^i_{S1}(\Omega) = \dfrac{1}{3}C_ST_0^3\displaystyle\int_0^{\theta^S_D/T_0}\frac{\Omega[\tau^C_S(x)]^2}{1 + [\Omega\tau^C_S(x)]^2}D(x)dx\\ \kappa^i_{S2}(\Omega) = \dfrac{1}{3}C_ST_0^3\beta_S\displaystyle\int_0^{\theta^S_D/T_0}\frac{\Omega\frac{[\tau^C_S(x)]^2}{\tau^N_S(x)}}{1 + [\Omega\tau^C_S(x)]^2}D(x)dx,\end{cases} \tag{17}$$

where $C_S = k_B^4/(2\pi^2\hbar^3 v_S)$, $(S = L, T)$, $D(x) = x^4 e^x/(e^x - 1)^2$ is Debye function, and θ_D^S is Debye temperature of the acoustic polarization branch S.[41] The partial conductivities κ_{S1} and κ_{S2} are the usual Debye-Callaway terms.[5,8]

C. Phonon scattering processes and their relaxation times

In SC crystals, phonons scattering processes can be divided into *intrinsic* processes arising from the anharmonicity of the interatomic forces, and *extrinsic* processes due to phonons scattering at the boundaries of the crystal and at various sorts of crystal defects and imperfections (e.g., point defects, impurities, dislocations, alloy disorder, grain boundaries, embedded nanoparticles, etc.) As first pointed out by Peierls,[1] anharmonic phonon scattering processes are of two distinct types, normal scattering processes (N-processes) which conserve the total crystal momentum after a collision, and Umklapp scattering processes (U-processes) for which the total crystal momentum changes by a reciprocal lattice vector after a collision. On the other hand, all extrinsic scattering processes do not conserve the total crystal momentum after a collision. Because of their conservative character of the total crystal momentum, N-processes cannot by themselves lead to a finite thermal conductivity. Consequently, as pointed out by Callaway,[5] it cannot be legitimate just to add scattering rates for N-processes to those which do not conserve the crystal momentum (U-processes and all extrinsic processes). The latter processes are called resistive scattering processes because at least one of them is needed to obtain a finite thermal conductivity. The effect of N-processes is addressed with a particular attention through the use of the displaced (*drifted*) Planck distribution as we have seen in Eq. (1).

In the single relaxation time approximation, as we have presented it in the above section, each scattering process is described by a relaxation time which naturally is a function of the phonon wave vector q and polarization S. It depends also on the nature of the scattering mechanism through coefficients characteristic of this mechanism. We, generally, express the relaxation times as functions of the phonon intrinsic frequency instead of the wave vector.[8] Depending on the nature of the scattering mechanism, relaxation times have different expressions. In our present analysis, we limit our discussion to four different scattering mechanisms, a phonon can undergo in a SC crystal. We use the forms of their relaxation times according to the approach of Morelli *et al.*,[18] in which every phonon scattering mechanism depends explicitly on the phonon mode. Moreover, we assume these forms to be the same for all studied SC crystals. Phonon scattering processes that are considered in our study are: (i) N-processes, (ii) U-processes, (iii) scattering of phonons by imperfections, and (iv) boundary scattering. The expressions of the scattering rates describing these processes are, respectively, given by[18]

$$\begin{cases} \begin{cases} [\tau_L^N(\omega)]^{-1} = B_N^L \omega^2 T^3, B_N^L = \dfrac{k_B^3 \gamma_L^2 V}{\hbar^2 M v_L^5} \\ [\tau_T^N(\omega)]^{-1} = B_N^T \omega T^4, B_N^T = \dfrac{k_B^4 \gamma_T^2 V}{\hbar^3 M v_T^5} \end{cases} & \text{(i)} \\ [\tau_S^U(\omega)]^{-1} = B_U^S \omega^2 \,\mathrm{Texp}(-\theta_D^S/3\mathrm{T}), B_U^S = \dfrac{\hbar \gamma_S^2}{M v_S^2 \theta_D^S} & \text{(ii)} \\ [\tau_S^i(\omega)]^{-1} = \dfrac{V\Gamma}{4\pi v_S^3}\omega^4 & \text{(iii)} \\ [\tau_S^B(\omega)]^{-1} = \dfrac{v_S}{L_C} & \text{(iv)}, \end{cases} \tag{18}$$

where γ_S, M, and V are the Grüneisen parameter for the phonon acoustic polarization branch S, the atomic mass, and the volume per atom, respectively. Depending on the temperature range, the crystallographic class and symmetry group of the SC crystal, different forms for normal and Umklapp scattering rates have been employed in literature to fit the experimental data of the steady-state thermal conductivity.[5,7–14,16–18,37,42,43]

In the case of scattering of phonons by imperfections, we assume scattering of phonons by natural isotopes in pure single SC crystals and by alloy disorder in SC crystal alloys. In both cases, the relaxation time is calculated assuming Rayleigh scattering regime valid, and the expression of the scattering rate as derived by Klemens[4] [Eq. (18ii) above]. Γ denotes the phonon scattering parameter that takes into account contributions from mass differences, atomic size differences, and bond strength differences between the impurity (imperfection) and the host lattice atom. Since we are treating the SC crystal as an elastic isotropic continuum medium, no much additional errors, would be introduced by neglecting the contribution of the differences in the atomic size and bond strength and considering only mass-difference contribution. In that case, Γ will represent the mass-fluctuation phonon scattering parameter.

The alloy is assumed to be a random mixture of atoms with different masses and volumes arranged in a lattice. In this case of alloy disorder scattering, Γ represents the disorder parameter and is calculated using the virtual lattice approach of Abeles.[9] According to this approximation, Γ of a mixture of two atoms A and B is given by[9]

$$\begin{cases} \Gamma = x(1-x)\left(\dfrac{\Delta M}{M}\right)^2 \\ \Delta M = M_A - M_B \\ M = xM_A + (1-x)M_B. \end{cases} \tag{19}$$

In the case of scattering of phonons due to the boundaries of the crystal, the scattering rate of this process is assumed to be independent of temperature and phonon dispersion for each acoustic phonon mode polarization S. L_C is a characteristic length of the crystal in the direction of the phonon transport. For all SC crystals considered in our study, we take L_C to be constant, $L_C = 5\,\mathrm{mm}$. The value of L_C is assumed to be long enough for the SC crystals to be treated as bulk materials.[18]

The inverse of the total resistive relaxation time τ_S^R accounting for all phonon scattering processes that destroy the total crystal momentum is given according to Mathiessen's rule

$$[\tau_S^R(\omega)]^{-1} = [\tau_S^U(\omega)]^{-1} + [\tau_S^i(\omega)]^{-1} + [\tau_S^B(\omega)]^{-1}. \quad (20)$$

III. RESULTS AND DISCUSSION

A. Behavior of the dynamical thermal conductivity

The physical picture we are interested in the current analysis is related to the behavior of the phonon gas in a region of the bulk SC crystal subject to a dynamical temperature gradient or a time or frequency dependent temperature disturbance resulting from the application of an external source.

In the theory section, we made the assumption that the Callaway pseudo-relaxation time β_S, describing the effect of N-processes, does not depend on time and that this approximation should preserve the essential features of the dynamical thermal conduction by phonons especially at temperatures above the maximum in the steady-state thermal conductivity ($T \approx 0.05\theta_D$). This assumption is plausible if one takes into consideration the smallness of $\boldsymbol{\lambda}_S$, but might be questionable at low temperatures and can eventually be relaxed to explore the effect of possible time dependence of β_S. We should note, however that, in their investigation of the conditions of manifestation of the second sound in solid dielectrics, Guyer and Krumhansl[29] gave a thorough discussion based on solving BPTE in the time domain where β_S was taken an explicitly time dependent function. The authors found that the dispersion relation of the second sound in solids obtained in both cases, with and without time dependent β_S, continues to exist with similar damping terms. This constitutes a robust argument to neglect the time dependence of β_S in our analysis. It is worthwhile to mention that in the simplest case of the GSA when all phonon modes belonging to a polarization branch S have the same relaxation times independent of the wave vector q, we can easily find that[5,8] $\beta_S = \tau_S^R$. This shows the very fundamental intertwining between anharmonic N-processes and resistive processes; the implicit effect of N-processes in the onset of a noninfinite thermal conductivity is taken account of through the resisting causing collisions namely the relaxation time of the resistive processes which effect is explicit.

The expression of the dynamical thermal conductivity $\kappa(\Omega)$ as given by Eq. (13) shows that $\kappa(\Omega)$ is an analytical function on the upper frequency complex plane. As a matter of fact, starting from the expressions of the real and imaginary parts $\kappa_r(\Omega)$ and $\kappa_i(\Omega)$ as given by Eq. (14), it is straightforward to show that these expressions are Hilbert transforms of each other, the Kramers-Kronig relations are then verified and as such the causality requirement is fulfilled where the dynamical temperature gradient is the driving potential force (*cause*) and the heat flux density current is the thermodynamically corresponding conjugate (*effect*).

When using the GSA, the expression of $\kappa(\Omega)$ reduces to

$$\kappa(\Omega) = \frac{\kappa_0}{1 - j\Omega\tau}, \quad (21)$$

where κ_0 is the steady-state thermal conductivity and τ is an effective wave vector independent relaxation time. Equation (21) is Cattaneo's expression of $\kappa(\Omega)$ which one can derive starting from BPTE in the GSA and solving directly in the frequency domain the moment equation giving the heat flux density current.

A very remarkable and interesting result that follows from Eq. (10) is obtained by going back to the time domain and performing an inverse Fourier transform; the latter transforms the natural product into a convolution product. The heat flux density current can be written in a convolution form in the real space-time domain as

$$\boldsymbol{J}_Q(x,t) = -\int_{-\infty}^{+\infty} K(t-t')\nabla T(x,t')dt' = -K \otimes \nabla T(x,t), \quad (22)$$

where "$\otimes$" represents the convolution product. Equation (22) says simply that the response at time t ($\boldsymbol{J}_Q$) is related to the previously applied driving potential force (∇T) as is required in all natural processes. The actual form of $\boldsymbol{J}_Q$ in Eq. (22) is similar to the form derived by Gurtin and Pipkin in their theory of heat conduction in solids in the linear regime,[44] where $K(t)$ is the heat flux relaxation function or *heat flux kernel* that takes the form

$$K(t) = \int_0^{\infty} \kappa(\Omega)e^{-j\Omega t}d\Omega = \sum_S \int \frac{1}{\tau_{\boldsymbol{q},S}^C} e^{-\frac{t}{\tau_{\boldsymbol{q},S}^C}} \kappa_{\boldsymbol{q},S}^0 d^3\boldsymbol{q}. \quad (23)$$

In order to discuss the behavior of the dynamical thermal conductivity $\kappa(\Omega)$ of bulk SC crystals, as a function of temperature as well as different intrinsic and extrinsic parameters, we consider 5 different SC in our analysis; (i) natural Si, (ii) natural Ge, (iii) $Si_{0.7}Ge_{0.3}$ alloy, (iv) $In_{0.53}Ga_{0.47}As$ alloy, and (v) $In_{0.49}Ga_{0.51}P$ alloy. The choice of these materials is based on their relevance and importance in microelectronic and optoelectronic industry especially in high frequency devices.[45,46] Besides $Si_{0.7}Ge_{0.3}$ alloy is known to be one of the best SC materials suited for thermoelectric energy conversion and more importantly in the thermoelectric generation process especially at high temperatures.[47]

Tables I and II recapitulate, respectively, the different geometrical and physical properties of the SC crystals used in our calculations. We assume all physical properties of the SC crystals to be independent of temperature. As we could not find documented values of Debye temperatures of $In_{0.53}Ga_{0.47}As$ and $In_{0.49}Ga_{0.51}P$ alloys in literature, we calculated them for both longitudinal and transverse acoustic phonon polarizations assuming the Debye cut-off frequency for each phonon mode to be given by $\omega_D^S = v_S q_D^S = v_S \pi/a$, where a is the SC lattice constant (see Table II).

When they are considered as fixed values, the Grüneisen parameters for longitudinal and transverse phonon acoustic polarization branches are taken to be the same for all single crystals and alloys; $\gamma_L = 1$ and $\gamma_T = 0.7$.[37]

Figure 1 shows the calculated behavior of the steady-state thermal conductivity $\kappa(0)$ of the 5 different bulk SC

TABLE I. Geometrical properties of the 5 bulk semiconductor crystals used in the simulation of the steady-state and dynamical behaviors of the thermal conductivity as a function of temperature and frequency of modulation of the introduced heat source.

Material	Lattice constant a (A)	Atomic mass M_a (kg) $\times 10^{-26}$	Volume per atom V (m^3) $\times 10^{-29}$	Density kg/m^3
Si	5.431	4.66	2	2329
Ge	5.658	12	2.27	5332
$Si_{0.7}Ge_{0.3}$	5.493	6.9	2.07	3332[a]
$In_{0.53}Ga_{0.47}As$	5.868	13.8	2.52	5500
$In_{0.49}Ga_{0.51}P$	5.653	10	2.24	4470

[a]Calculated based on the properties of individual elements at $T = 300$ K considering the (100) direction.[48]

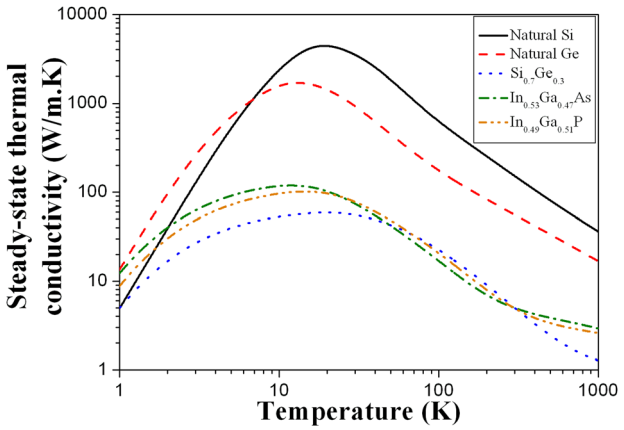

FIG. 1. Computed behavior of the steady-state thermal conductivity $\kappa(0)$ of the 5 different bulk SC crystals as a function of temperature.

crystals as a function of temperature. A typical bell-shape behavior is reproduced, in which $\kappa(0)$ follows an almost T^3 power law behavior at low temperatures, reaches a maximum then starts to fall off at high temperatures due mainly to anharmonic phonon-phonon scattering processes.[5–18] The peak value of $\kappa(0)$ of each SC material is found to be achieved for a temperature of about ($T \approx 0.06\theta_D$) in agreement with the aforementioned estimation in the introduction, where θ_D is an average Debye temperature over longitudinal and transverse acoustic branches $\theta_D = (\theta_D^L + 2\theta_D^T)/3$. $Si_{0.7}Ge_{0.3}$ alloy shows the lowest peak value of $\kappa(0)$. The calculated T-behavior of $\kappa(0)$ is in a very good agreement with reported experimental data for all 5 bulk SC crystals; Si and Ge,[13,14,17,18] $Si_{0.7}Ge_{0.3}$, $In_{0.53}Ga_{0.47}As$, and $In_{0.49}Ga_{0.51}P$.[37,50]

In Figs. 2(a) and 2(b), we report, respectively, the calculated behaviors of the real part and amplitude of the dynamical thermal conductivity $\kappa(\Omega)$ for the 5 different bulk SC crystals at room temperature, over a frequency interval [0.1 Hz–160 THz]. The insets in Figs. 2(a) and 2(b) illustrate the behaviors of the imaginary part and phase of $\kappa(\Omega)$, respectively. As expected, the amplitude of $\kappa(\Omega)$ shows a plateau in the low frequency regime and then starts to fall off rapidly as the frequency gets higher; a typical first order low-pass filter thermal behavior. The phonon gas cannot follow the thermal perturbation when the frequency of the latter becomes very high; the SC crystal becomes a thermal insulator. We can see also that the beginning of the falling off occurs at different threshold frequencies depending on the SC crystal; the SC alloy crystals seem to be characterized by lower threshold frequencies than the single SC crystals. The inset in Fig. 2(a) shows the frequency behavior of the imaginary part $\kappa_i(\Omega)$. The latter manifests a Lorentzian-shape behavior describing a resonance phenomenon of the phonon gas in the SC crystal at a resonance frequency $f_R = 1/2\pi\tau_m$, where τ_m is a certain weighted average relaxation time over all phonon scattering mechanisms and polarizations. SC alloy crystals are characterized by lower resonance amplitudes than single SC crystals. On the other hand, the inset in Fig. 2(b) shows the phase of $\kappa(\Omega)$ increasing as a function of frequency to saturate at a value of $\pi/2$ in the high frequency regime. This is also a typical behavior of the phase that describes the delay between the cause (dynamical temperature gradient) and the effect (heat flux density current) in a first order linear system.

Because of the important role, $Si_{0.7}Ge_{0.3}$ SC alloy plays in thermoelectricity as well as in microelectronics, we consider this SC crystal as a test bulk material to study the effect

TABLE II. Physical properties of the 5 bulk semiconductor crystals used in the simulation of the steady-state and dynamical behaviors of the thermal conductivity as a function of temperature and frequency of modulation of the introduced heat source.

Material	Longitudinal sound velocity v_L (m/s)	Transverse sound velocity v_T (m/s)	Longitudinal Debye temperature θ_{DL} (K)	Transverse Debye temperature θ_{DT} (K)	Longitudinal Grüneisen parameter γ_L	Transverse Grüneisen parameter γ_T	Rayleigh mass-fluctuation phonon-scattering parameter Γ
Si	8430[a]	5840[a]	586[a]	240[a]	1[b]	0.7[b]	2×10^{-4}[a]
Ge	4920[a]	3540[a]	333[a]	150[a]	1[b]	0.7[b]	6.08×10^{-4}[a]
$Si_{0.7}Ge_{0.3}$	6812[c]	4769[c]	510[d]	213[d]	1[b]	0.7[b]	0.2403[f]
$In_{0.53}Ga_{0.47}As$	4267[c]	2984[c]	175[e]	122[e]	1[b]	0.7[b]	0.0357[b]
$In_{0.49}Ga_{0.51}P$	5208[c]	3609[c]	221[e]	153[e]	1[b]	0.7[b]	0.0675[b]

[a]Reference 18.
[b]Reference 37.
[c]Calculated based on the properties of individual elements at $T = 300$ K considering the (100) direction.[48]
[d]Calculated using the weighted average approach from Ref. 49.
[e]Calculated from the sound velocities assuming the Debye cut-off wave vector $= \pi/a$, where a is the lattice constant: $\theta_D^S = \hbar v_S q_D^S / k_B$ with $q_D^S = \pi/a \Rightarrow \theta_D^S = h v_S / 2k_B a$.
[f]Calculated using the virtual medium approach from Ref. 9.

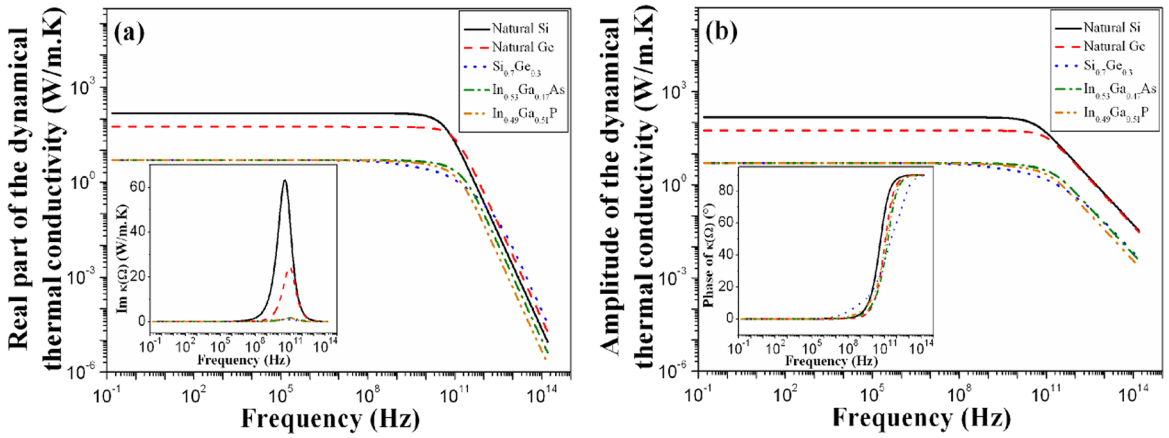

FIG. 2. Computed behavior of the dynamical thermal conductivity $\kappa(\Omega)$ of the 5 different bulk SC crystals at room temperature as a function of frequency. (a) Real part (imaginary part in the inset) and (b) amplitude (phase in the inset).

of changing temperature as well as different intrinsic and extrinsic parameters on the behavior of $\kappa(\Omega)$. The first parameter to consider is temperature. We report, respectively, in Figs. 3(a) and 3(b) the calculated dynamical behaviors of the real part and amplitude of $\kappa(\Omega)$ of $Si_{0.7}Ge_{0.3}$ SC bulk alloy at different temperatures. While the low frequency regime behavior mirrors the steady-state behavior, we can see that at each temperature, the values of the thermal conductivity in the high frequency regime are reduced drastically in comparison with the low frequency regime values, so that the SC alloy becomes almost a perfect thermal insulating material. For instance, at $T = 300\,\mathrm{K}$, the amplitude of $\kappa(\Omega)$ decreases by almost 3 orders of magnitude when it is compared to the reference bulk value of $\sim 5\,\mathrm{W/m\ K}$. As the temperature increases, the reduction rate decreases and the deviation threshold frequency from the plateau shape increases, which

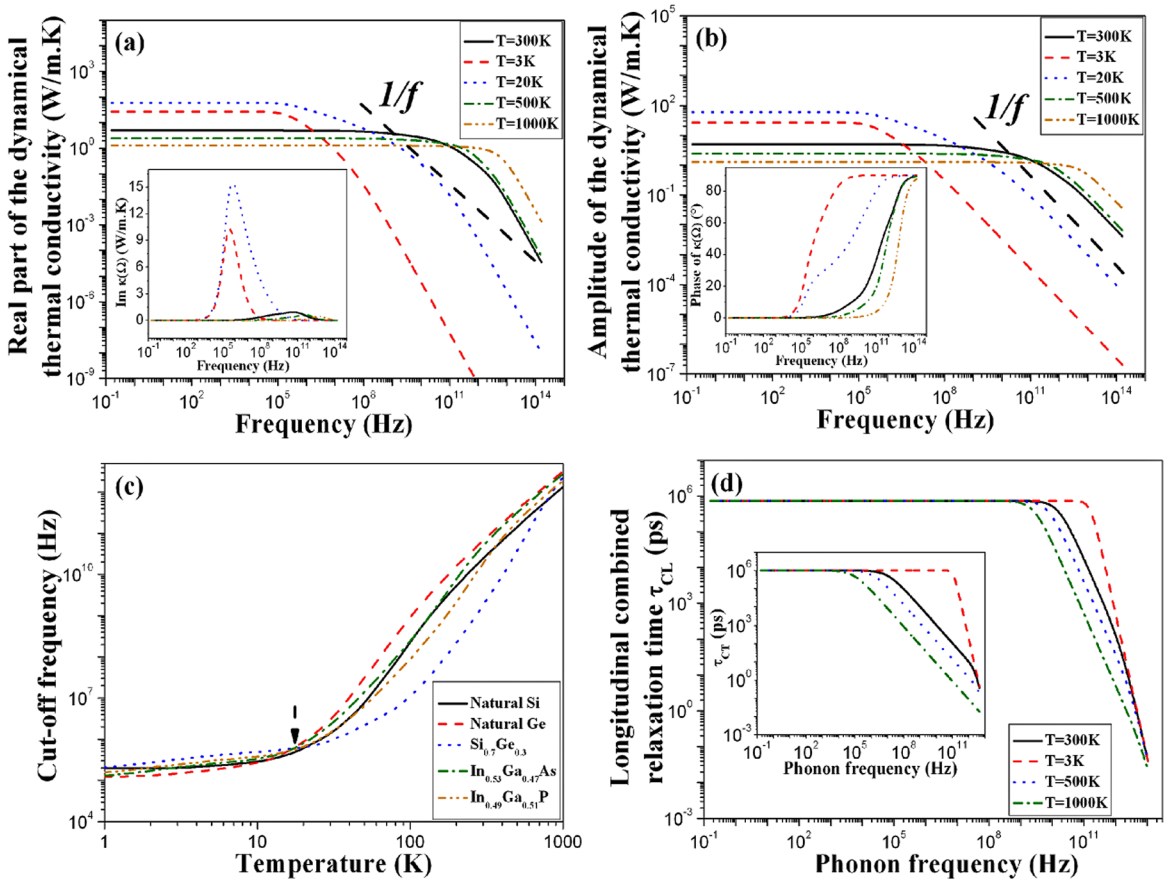

FIG. 3. (a) Computed behavior of the real part $\kappa_r(\Omega)$ of the dynamical thermal conductivity $\kappa(\Omega)$ of $Si_{0.7}Ge_{0.3}$ SC alloy as a function of frequency for different temperatures T, the inset shows the imaginary part $\kappa_i(\Omega)$. (b) Computed behavior of the amplitude of $\kappa(\Omega)$ of $Si_{0.7}Ge_{0.3}$SC alloy as a function of frequency for different T, the inset shows the phase. (c) Computed behavior of the cut-off frequency f_C of $\kappa(\Omega)$ for the 5 different bulk SC crystals as a function of T. (d) Computed behavior of the combined relaxation time τ_S^C in the case of $Si_{0.7}Ge_{0.3}$SC alloy, for both longitudinal and transverse (inset) acoustic phonon polarization branches, as a function of the intrinsic phonon frequency ω and at different T.

leads to an increase of the cut-off frequency f_C of $\kappa(\Omega)$ as a function of temperature. As it is customary in microelectronics, f_C is defined as the frequency at which $Amp[\kappa(f_C)] = Max\{Amp[\kappa(f)]\}/\sqrt{2} = \kappa(0)/\sqrt{2}$ and can formally be expressed as $f_C = 1/2\pi\tau_m^C(\omega_D^L, \omega_D^T)$, where τ_m^C is a weighted average combined relaxation time of τ_L^C and τ_T^C evaluated at the cut-off Debye frequencies ω_D^L and ω_D^T, respectively. Even though it is not really systematic, but we can always find a relation between τ_m and τ_m^C that relates the position of the resonance peak in the imaginary part $\kappa_i(\Omega)$ to f_C of $\kappa(\Omega)$. Fig. 3(c) reports the behavior of f_C as a function of temperature for the 5 SC bulk crystals considered in our study, and Fig. 3(d) illustrates the behavior of the combined relaxation time τ_S^C [Eq. (7)] in the case of $Si_{0.7}Ge_{0.3}$ SC alloy, for both longitudinal and transverse (inset) acoustic phonon polarization branches, as a function of the intrinsic phonon frequency ω (dispersion relation) and at different temperatures. Over the temperature range considered in our analysis [1–1000 K], $f_C(T)$ shows similar trends for all 5 SC bulk crystals and it increases as the temperature is increased. It seems that there is a threshold temperature in the $f_C(T)$ behavior at which the increasing rate of f_C suddenly gets faster. A simple look to Fig. 1 suggests that this threshold point in the $f_C(T)$ behavior corresponds to the temperature value at which the steady-state thermal conductivity $\kappa(0)$ reaches a maximum. This interesting feature might be attributed to the interplay between all phonon scattering processes that take place at this particular temperature for each SC crystal. We can see also that for all 5 SC crystals, f_C varies from 100 kHz up to few THz. f_C of $Si_{0.7}Ge_{0.3}$ SC alloy shows an interesting trend; it has the highest increasing rate as a function of temperature among all 5 SC crystals for $T \leq 20$ K, then this rate becomes the lowest for $20 \leq T \leq 770$ K. For this SC alloy, f_C is as low as 12 MHz at $T = 100$ K and is still less than 2 GHz at room temperature ($T = 300$ K). Even at a temperature as high as $T = 600$ K, f_C is still less than 100 GHz, this latter value will be soon within the reach of high frequency microelectronic devices according to the ITRS.[28] The very low value of f_C in the low T regime indicates that the dominant mean relaxation time of phonon scattering in this regime is on the order of microseconds. These results shed light on how crucial and critical understanding the dynamical behavior of the thermal conductivity has become, in order to better control energy and heat transport in low and high operating temperature microelectronic and optoelectronic devices.

In contrary to the high frequency behavior of the real part, the high frequency behavior of the amplitude can be fitted with a very satisfying f^{-1} power law at each temperature. This confirms the previous analysis of Volz[33] who found the same asymptotic behavior in his study of $\kappa(\Omega)$ of silicon using molecular dynamics method based on spectral Green-Kubo approach.[33] The f^{-1} power law is expected to be valid in the behavior of the amplitude of $\kappa(\Omega)$ for $f \geq f_C$. As a matter of fact, in the high frequency regime, the transport of phonons is predominantly ballistic, this leads to a relaxation time independent response, for which the temperature dependence is mostly governed by the specific heat temperature dependence, i.e., low temperature quantum effect, as discussed earlier by Volz,[33] and the acoustic velocity captures the dynamics.

The low operating temperature regime where long wavelength phonons dominate is known to be a place where very interesting and a variety of fundamental phonon transport phenomena occur, particularly ballistic phonon transport and second sound propagation in which the interplay between anharmonic phonon-phonon scattering N-processes and U-processes plays a key role.[29] Low cut-off frequency of $\kappa(\Omega)$ is another phenomenon to be added to the list, and might be fundamentally connected to both aforementioned phenomena.

The frequency behavior of the imaginary part and the phase of $\kappa(\Omega)$ are reported in the insets of Figs. 3(a) and 3(b), respectively. By decreasing temperature, both the position of the resonance peak and its amplitude change; in a way these changes mirror the behavior of the steady-state thermal conductivity as a function of temperature. On the other hand, the phase seems to increase and reach the saturation value of $\pi/2$ faster as the temperature decreases.

Among the extrinsic parameters that we consider the effect of their variations on $\kappa(\Omega)$, we have both longitudinal and transverse Grüneisen parameters γ_L and γ_T as well as the mass-fluctuation parameter Γ. We report, respectively, in Figs. 4(a) and 4(b) the calculated dynamical behaviors at room temperature of the real part and the amplitude of $\kappa(\Omega)$ of $Si_{0.7}Ge_{0.3}$ SC alloy for different values of γ_L while in Figs. 4(c) and 4(d), we report, respectively, the dynamical behaviors of the same functions for different values of γ_T. The insets in Figs. 4(a) and 4(c) illustrate the behavior of the imaginary part of $\kappa(\Omega)$. On the other hand, the behavior of the phase of $\kappa(\Omega)$ is illustrated in the insets of Figs. 4(b) and 4(d). Rigorously speaking, the mode Grüneisen parameters γ_L and γ_T depend on the phonon intrinsic frequency (dispersion relation). Depending on the SC crystal crystallographic class and symmetry group, γ_L and γ_T can be calculated using *ab-initio* lattice dynamical models.[18]

In our analysis, we consider the average values of γ_L and γ_T to vary from 0.5 to 1.5 and from 0.2 to 1.2, respectively. We remind here that in previous figures we assumed fixed values of $\gamma_L = 1$ and $\gamma_T = 0.7$ in our calculations. By varying the Grüneisen parameter, the strengths of both anharmonic phonon-phonon U-processes and N-processes scattering rates change. According to Eqs. (18i) and (18ii), both scattering rates strengths have a quadratic dependence on the value of the Grüneisen parameter.

As can be seen in Figs. 4(a)–4(d), changing γ_L (respectively, γ_T) seems to have an effect mainly in the low frequency regime and particularly near the resonance frequency in the behavior of the imaginary part, while no significant effect occurs in the high frequency regime where all curves almost collapse. By decreasing γ_L (resp. γ_T), the strength of the scattering rate of both N-processes and U-processes decreases which lead to an increase in the amplitude of $\kappa(\Omega)$ in the low frequency regime, this effect mirrors again the effect of changing γ_L (respectively, γ_T) on the steady-state thermal conductivity where the effect is manifested for temperatures above the maximum and completely disappear for temperatures below [Fig. 4(g) for γ_L and Fig. 4(h) for γ_T].

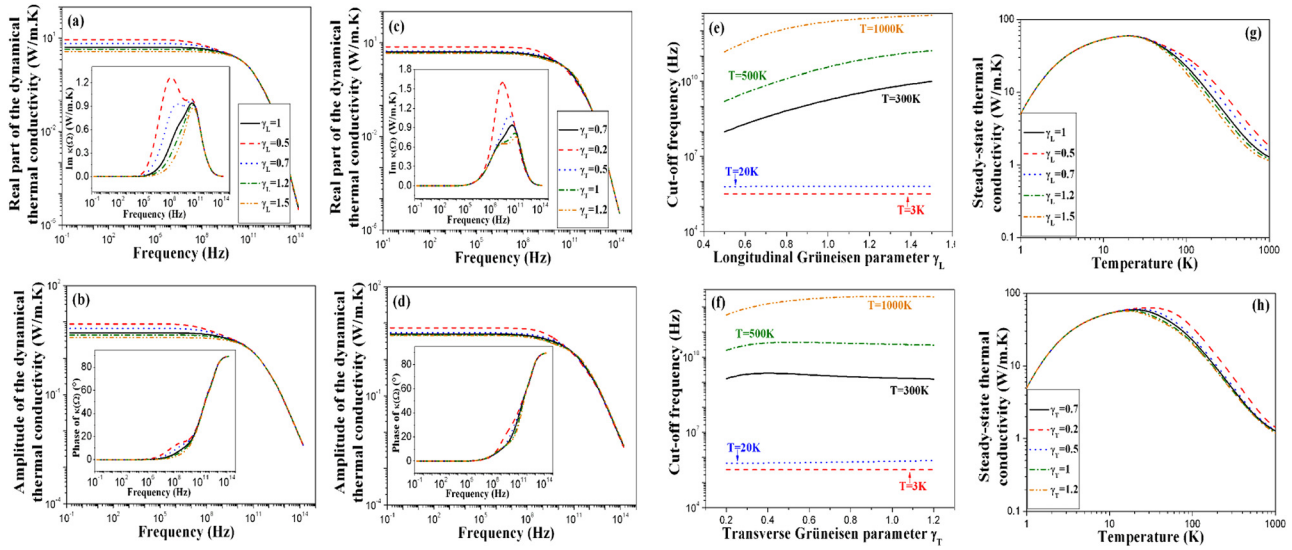

FIG. 4. Computed behavior of the real part $\kappa_r(\Omega)$ ((a) and (c)) and amplitude ((b) and (d)) of $\kappa(\Omega)$ of $Si_{0.7}Ge_{0.3}$ SC alloy at room temperature as a function of frequency for different values of the (longitudinal, transverse) Grüneisen parameter (γ_L, γ_T). The insets in (a) and (c) show the imaginary part $\kappa_i(\Omega)$, while the insets in (b) and (d) show the phase. Computed behavior of f_C of $\kappa(\Omega)$ of $Si_{0.7}Ge_{0.3}$SC alloy as a function of γ_L (e) and γ_T (f) for different T. Computed behavior of $\kappa(0)$ of $Si_{0.7}Ge_{0.3}$ SC alloy as a function of T for different values of γ_L (g) and γ_T (h).

Probably the most interesting and intriguing effect of varying γ_L (resp. γ_T) is illustrated in the dynamical behavior of the imaginary part $\kappa_i(\Omega)$, and may be less importantly in the behavior of the phase. For both functions, the effect occurs on the same frequency interval. A double resonance peak shape seems to appear in $\kappa_i(\Omega)$ as we decrease γ_L, while the same effect happens by increasing γ_T. On the other hand, the amplitude of the resonance peak increases by decreasing either γ_L or γ_T.

In Figs. 4(e) and 4(f), we report the behavior of the cut-off frequency f_C of $\kappa(\Omega)$ as a function of γ_L and γ_T, respectively, for different temperatures T. At low T, f_C is almost constant independent of γ_L (respectively, γ_T), and as long as we increase T, different behaviors of f_C start to occur. In the high T regime, f_C keeps increasing as γ_L increases, while for increasing γ_T, f_C seems to reach quickly a saturation value that increases with T.

The effects of varying γ_L and γ_T on $\kappa(\Omega)$ and particularly on $\kappa_i(\Omega)$ capture the essence of the fundamental interplay between anharmonic phonon-phonon scattering N-processes and U-processes.

In Figs. 5(a) and 5(b) we report, respectively, the calculated dynamical behavior at room temperature of the real part $\kappa_r(\Omega)$ and the steady-state behavior of $\kappa(0)$ of $Si_{0.7}Ge_{0.3}$

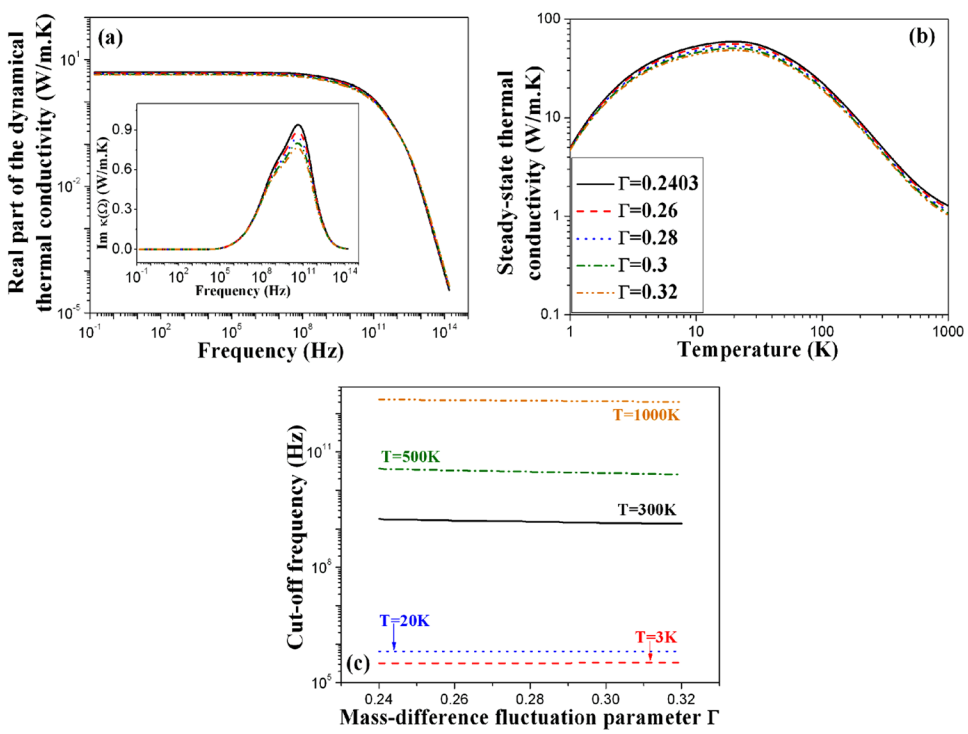

FIG. 5. (a) Computed behavior of the real part $\kappa_r(\Omega)$ of $Si_{0.7}Ge_{0.3}$ SC alloy at room temperature as a function of frequency for different values of the mass-difference fluctuation parameter Γ, the inset shows the imaginary part $\kappa_i(\Omega)$. (b) Computed behavior of $\kappa(0)$ of $Si_{0.7}Ge_{0.3}$ SC alloy as a function of temperature T for the same different values of Γ. (c) Computed behavior of f_C of $\kappa(\Omega)$ of $Si_{0.7}Ge_{0.3}$SC alloy as a function of Γ for different T.

SC alloy for different values of the mass-fluctuation parameter Γ. Γ is assumed to change from its initial alloy disorder value of $\Gamma \approx 0.24$ to $\Gamma = 0.36$. Increasing Γ can be obtained by isotopically enriching the SC alloy and/or incorporating additional impurities. The inset of Fig. 5(a) illustrates the dynamical behavior of the imaginary part $\kappa_i(\Omega)$. Varying Γ does not seem to have a significant effect on the behavior of the three functions; neither does it on the behavior of the cut-off frequency f_C, the behavior of which as a function of Γ for different temperatures is reported in Fig. 5(c). At each temperature, f_C is almost a constant independent of Γ and increases as one increases T [Fig. 3(c)].

Another extrinsic parameter that deserves to be considered is scattering of phonons by embedded foreign nanoparticles. This concept has been proven to be very effective in reducing the steady-state thermal conductivity in SC crystal alloys.[49] The study of the effect of embedding SC nanoparticles on the dynamical behavior of $\kappa(\Omega)$ of SC crystal alloys is underway and will be presented in a future work.

B. Koh and Cahill experimental results

In a very recent experiment, Koh and Cahill[37] published very interesting and intriguing experimental results of the frequency behavior of the thermal conductivity of SC crystal alloys at different ambient temperatures. As we mentioned in the introduction, Koh and Cahill's results over the frequency range used in their experiments [0.6–10 MHz] show $\kappa(\Omega)$ of SC alloys to have a cut-off frequency $f_C < 10$ MHz, while $\kappa(\Omega)$ of single SC crystals manifested a plateau at room temperature. As we mentioned in the introduction, the authors used BPTE in the steady-state regime to explain their results in which they translate *Koh and Cahill statement* (see Introduction) as a boundary scattering process that phonons would undergo at a virtual interface. This virtual interface is actually the surface of a hemisphere whose radius is the thermal penetration depth $\delta(\Omega)$. The authors found a satisfactory agreement between experimental data and the results of this phenomenological approach.

Even though their model seems to agree with experimental data, but it cannot be considered as a relevant and robust explanation of the behavior of $\kappa(\Omega)$ of SC crystals and that for two reasons: (i) the thermal penetration depth δ is a characteristic depth of the applied heat source at the surface of the crystal which is calculated based on the knowledge of the thermal diffusivity (related to the thermal conductivity) of the given crystal and the frequency of the heat source, and then cannot be considered as a limit for phonon MFP inside the crystal, this raises a consistency question. (ii) There is no physically plausible reason to consider scattering of phonons at a fictitious interface.

Koh and Cahill experimental results are very low compared to the predicted values of f_C based on the above modeling of $\kappa(\Omega)$. Furthermore, a value of $f_C = 10$ MHz at room temperature is equivalent to a relaxation time of the dominant phonon scattering process of $\tau \sim 16$ ns, this is a very large value and it is hard to be accepted physically; besides, it is difficult to admit that $\kappa(\Omega)$ of bulk SC alloys will undergo such a huge reduction on a small frequency range. The most reasonable explanation to the measured low value of f_C in SC crystal alloys in Koh and Cahill's experiment[37] would be related to the physical meaning of the measured thermal conductivity κ itself and the role of the cumulative effect of the laser train pulses in the experimental setup and thermal modeling assumptions used to extract κ especially at high frequency of the excitation source. The recent experiments of Minnich *et al.*[51,52] take the same reasoning direction and come to support this conclusion, where the authors used again TDTR technique to study quasiballistic heat transport and to measure phonon MFP. The results of the authors show the measured thermal conductivity κ to depend on the size of the heating laser pump source spot and it is independent of the modulation frequency of the latter.

Koh and Cahill experimental results are still intriguing and deserve much more investigation. It is more plausible that, in the experiment, the authors measured an *apparent thermal conductivity* κ_{app} that matches the real intrinsic κ at low frequency but deviates from it as the frequency of the excitation source gets higher due mainly to the cumulative effect of the TDTR experimental set-up and thermal modeling assumptions.[38–40] We believe these two factors need further study to separate their effect from the measured κ_{app} in order to have access to the real intrinsic thermal conductivity of the studied dielectric crystal.

C. Shastry's sum rule

In this last subsection, we will shed light on a very interesting result that has been recently introduced by Shastry,[35] namely the sum-rule for the real part of the dynamical thermal conductivity. Shastry derived this sum rule for several standard models of current interest in condensed matter. The sum rule is obtained using standard linear response theory and is expressed in terms of the expectation of an extensive object θ^{xx} that Shastry named "*thermal operator*" in his formalism.[35] As discussed by Shastry, the sum rule is closely related to the behavior of energy (heat) transport in the ballistic regime where the expectation of θ^{xx} is an equilibrium value that determines the magnitude of the ballistic force exerted by the applied temperature field.[36] Here, we study the applicability of SSR and we develop rather "*classical*" expressions for it as well as the expectation of θ^{xx} in the case of the dynamical lattice thermal conductivity $\kappa(\Omega)$ of bulk SC crystals as calculated based on BPTE for phonon transport.

According to the calculations developed earlier in the theory section, we can calculate the integral of the real part of $\kappa(\Omega)$. We will consider two cases of anharmonic phonon-phonon scattering processes; (i) both normal and Umklapp processes are included and (ii) only Umklapp process is active. In both cases of course, in addition to the above mentioned phonons scattering processes, all other total phonon crystal momentum destroying processes are taken into account. The integral is taking over all frequencies from zero to infinity. In the first case [Eqs. (11)–(14)], one obtains

$$\int_0^{+\infty} \kappa_r(\Omega)d\Omega = \sum_S \int \kappa^0_{\boldsymbol{q},S} \left[\int_0^{+\infty} \frac{d\Omega}{1+(\Omega\tau^C_{\boldsymbol{q},S})^2} \right] d^3\boldsymbol{q} = \frac{\pi}{2}\sum_S \int \frac{\kappa^0_{\boldsymbol{q},S}}{\tau^C_{\boldsymbol{q},S}} d^3q$$
$$= \frac{1}{48\pi^2}\sum_S \int \left[1+\frac{\beta_S}{\tau^N_{\boldsymbol{q},S}}\right] v_S^2 C_{Ph}(\boldsymbol{q},S)d^3\boldsymbol{q}. \quad (24)$$

Since the result function depends on phonons scattering rates due to the term $\beta_S/\tau^N_{\boldsymbol{q},S}$ (effect of N-processes), it cannot be viewed as a sum rule; as explained by Shastry,[35] the thermal operator θ^{xx} does not contain any scattering rate. On the other hand, when N-processes are disregarded and only resistive processes are considered, we can easily show that the calculation of the integral of the real part of $\kappa(\Omega)$ gives

$$\int_0^{+\infty} \kappa_r(\Omega)d\Omega = \frac{1}{8\pi^3}\sum_S \int \tau^R_{\boldsymbol{q},S} v^2_{S,t} C_{Ph}(\boldsymbol{q},S) \left[\int_0^{+\infty} \frac{d\Omega}{1+(\Omega\tau^R_{\boldsymbol{q},S})^2} \right] d^3\boldsymbol{q}$$
$$= \frac{1}{16\pi^2}\sum_S \int v^2_{S,t} C_{Ph}(\boldsymbol{q},S)d^3\boldsymbol{q}$$
$$= \frac{\pi}{6}\sum_S \int_0^{\omega_D^S} v_S^2 C_{Ph}(\omega,S) g_S(\omega)d\omega, \quad (25)$$

where $g_S(\omega) = \omega^2/(2\pi^2 v_S^3)$ is Debye density of states of phonons in the acoustic polarization branch S.[41] This last expression shows that the result function is independent of any phonons scattering rate and hence can be viewed as a sum rule. Comparison of Eq. (25) to Eq. (17) from Shastry's paper[35] implies that the classical expression of the expectation of the thermal operator θ^{xx} can be written as

$$\frac{1}{\hbar}\langle\theta^{xx}\rangle^{BPTE}_{Classical} = \frac{2T_0 W}{\pi}\int_0^{+\infty} \kappa_r(\Omega)d\Omega$$
$$= \frac{T_0 W}{3}\sum_S \int_0^{\omega_D^S} v_S^2 C_{Ph}(\omega,S) g_S(\omega)d\omega, \quad (26)$$

where W denotes the total volume of the SC crystal material. Then using the usual change of variable $x = \hbar\omega/k_B T_0$, one can further write (26) in a more convenient form for numerical calculation, this gives

$$\langle\theta^{xx}\rangle^{BPTE}_{Classical} = \frac{k_B^4}{\pi^2\hbar^2} W T_0^4 \left\{ \frac{1}{6v_L}\int_0^{\theta_D^L/T_0} D(x)dx + \frac{1}{3v_T}\int_0^{\theta_D^T/T_0} D(x)dx \right\}, \quad (27)$$

where again $D(x)$ denotes Debye function.

The expression of $\langle\theta^{xx}\rangle^{BPTE}_{Classical}$ as given by Eq. (27) presents the remarkable feature of vanishing at $T=0$ (i.e., in the true thermodynamic ground state). This finding corroborates the arguments of Shastry who discussed this fundamental behavior and showed its deep connection to the vanishing of the lattice specific heat.[35] As a matter of fact, starting from the definition of the latter thermodynamic property, in our case the lattice specific heat at constant volume C_W, it is straightforward to show that it has the following expression:[6,16,41]

$$C_W(T_0) = \sum_S \int_0^{\omega_D^S} C_{Ph}(\omega,S) g_S(\omega)d\omega$$
$$= \frac{k_B^4}{2\pi^2\hbar^3} T_0^3 \left\{ \frac{1}{v_L^3}\int_0^{\theta_D^L/T_0} D(x)dx + \frac{2}{v_T^3}\int_0^{\theta_D^T/T_0} D(x)dx \right\}. \quad (28)$$

Comparison of Eqs. (27) and (28) shows clearly the connection between $\langle\theta^{xx}\rangle^{BPTE}_{Classical}$ and C_W. As a matter of fact, one can write

$$\begin{cases} \dfrac{\langle\theta^{xx}\rangle^{BPTE}_{Classical}}{\hbar T_0 W} = \dfrac{1}{3} C_W v^2_{eff} \\ v^2_{eff} = \dfrac{\left\{ \dfrac{1}{v_L}\displaystyle\int_0^{\theta_D^L/T_0} D(x)dx + \dfrac{2}{v_T}\int_0^{\theta_D^T/T_0} D(x)dx \right\}}{\left\{ \dfrac{1}{v_L^3}\displaystyle\int_0^{\theta_D^L/T_0} D(x)dx + \dfrac{2}{v_T^3}\int_0^{\theta_D^T/T_0} D(x)dx \right\}} \end{cases}, \quad (29)$$

where v_{eff} represents an effective phonon group velocity averaged over all phonon acoustic polarization branches.

The fact that $\langle\theta^{xx}\rangle^{BPTE}_{Classical}$ and C_W can be related by such a compact formula [Eq. (29)] that is similar to the one suggested by Shastry [Eq. (91) in Ref. 35] proves somehow the meaningfulness of the classical limit of the expectation of the thermal operator θ^{xx} and confirms the physical meaning of the latter variable in capturing the ballistic dynamics aspect in the energy (heat) transport phenomenon.

Based on this short analysis of the sum rule within the frame work of Boltzmann-Peierls theory of phonon transport using the single relaxation time approximation with Callaway approximated form of the collision operator, N-processes appear to play a very fundamental role in capturing the dynamics of energy (heat) transport in SC crystals. Through their role of shuffling the total phonon crystal momentum between different phonon states, N-processes have always to be considered in any study of phonon transport. The fact that taking them into account within the above framework with time independent Callaway parameter, leads to a breakdown of the sum rule of the real part of $\kappa(\Omega)$, constitutes a very interesting finding regarding phonon transport phenomena in SC crystals that needs to be checked using more sophisticated and complete modeling of energy and heat transport in these dielectric materials using first principles calculations and atomistic *ab-initio* Green's function approaches.[53]

IV. SUMMARY AND CONCLUDING REMARKS

Using BPTE with Callaway approximated form of the collision operator and time independent Callaway parameter, we have derived a compact expression for the dynamical lattice thermal conductivity $\kappa(\Omega)$ of bulk SC crystals. This expression of $\kappa(\Omega)$ captures the leading behavior and the essential features of the dynamical thermal conduction by phonons. It fulfils the causality requirement and leads to a convolution type relationship between the heat flux density current and the temperature gradient in the real space-time domain in agreement with Gurtin-Pipkin theory. We considered the study of the effect of temperature as well as different intrinsic and extrinsic parameters. Our calculations confirm previous theoretical studies regarding the order of magnitude of the cut-off frequency f_C of $\kappa(\Omega)$ and further show f_C to be very sensitive to the variation of temperature and Grüneisen parameter. On the other hand, varying the mass-fluctuation parameter seems to have no effect on f_C. Low values of f_C in the low temperature regime, is another manifestation of the ballistic phonon transport regime in which the intertwining between anharmonic phonon-phonon scattering N-processes and U-processes plays a key role.

Our model is unable, however, to explain Koh and Cahill puzzling experimental results and one needs to conduct more experiments in order to check the relevance of the calculations results and shed light on the eventual discrepancies.

The applicability of SSR to $\kappa(\Omega)$ revealed anharmonic phonon-phonon N-processes to play a very fundamental role in capturing the dynamics of energy (heat) transport in SC crystals. We found that SSR holds only when these phonon scattering processes are disregarded and only resistive phonon scattering processes are considered. In this latter case, we were able to extract a classical expression to the expectation of the thermal operator θ^{xx} introduced by Shastry. This expression preserves the deep connection linking the expectation of this operator to the lattice specific heat, namely the vanishing in the true thermodynamic ground state (i.e., at $T=0$), as already discussed by Shastry. It also confirms the physical meaning of θ^{xx} variable in capturing the ballistic dynamics aspect in the energy (heat) transport phenomenon.

The treatment outlined forth in the theory section highlights the leading dynamical behavior of $\kappa(\Omega)$ and it allows us to have a consistent and meaningful classical limit of SSR, nevertheless this treatment of BPTE within the framework of a single relaxation time cannot be considered as fully rigorous as it depends on few assumptions that can eventually be relaxed. Therefore, many improvements can be contemplated in order to check the relevance and consistency of some of the calculations results we presented above, regarding particularly the behavior of the cut-off frequency f_C of the dynamical thermal conductivity $\kappa(\Omega)$ as a function of temperature T and Grüneisen parameter. The improvements would be related to:

1. The form of the collision operator including the separate effect of anharmonic N-processes and U-processes.
2. The effect of specularity in phonon boundary scattering especially in the low temperature regime. We have considered a fixed characteristic length L_C in our analysis; changing L_C would affect the behavior of $\kappa(0)$ and $\kappa(\Omega)$ enormously in this low T regime.
3. The phonon wave vector dependence of the expressions of all phonon scattering rates, particularly N-processes and U-processes. In this case, a complete modeling using first principles calculations and atomistic *ab-initio* Green's function approaches will be very helpful and will allow to treat intrinsic and extrinsic phonon scattering mechanisms more respectfully including any eventual contribution from optical phonons especially in the high T regime.
4. The explicit time dependence of Callaway parameter β when approximated Callaway form of the collision operator is used as we did in our analysis except that we assumed $\beta = cte$ independent of time in our treatment. In this case of time dependent β, the mathematical treatment of BPTE would be a bit tedious in which it would be easier to solve the problem directly in the time domain following the approach of Guyer and Krumhansl and using the trajectory integral method. We plan to investigate this approach in a future work in order to study the impact on the behavior of f_C of $\kappa(\Omega)$ as function of T (it is more likely that f_C would be a little bit lower than what we expected above especially in the low T regime) as well as the applicability of SSR and the causality requirement when N-processes are turned on.

ACKNOWLEDGMENTS

We are deeply thankful to Professor Ali Shakouri for his enlightening and fruitful discussions throughout this work.

[1]R. E. Peierls, Ann. Phys. (Leipzig) **3**, 1055 (1929).
[2]P. G. Klemens, Proc. R. Soc. London, Ser. A **208**, 108 (1951).
[3]C. Herring, Phys. Rev. **95**, 954 (1954).
[4]P. G. Klemens, Proc. Phys. Soc., London, Sect. A **68**, 1113 (1955).
[5]J. Callaway, Phys. Rev. **113**, 1046 (1959).
[6]J. M. Ziman, *Electron and Phonons* (Oxford University Press, New York, 1960).
[7]J. Callaway, Phys. Rev. **122**, 787 (1961).
[8]P. Carruthers, Rev. Mod. Phys. **33**, 92 (1961).
[9]B. Abeles, Phys. Rev. **131**, 1906 (1963).
[10]R. E. Nettleton, Phys. Rev. **132**, 2032 (1963).
[11]M. G. Holland, Phys. Rev. **132**, 2461 (1963).
[12]G. A. Slack and S. Galginaitis, Phys. Rev. **133**, A253 (1964).
[13]G. A. Slack and C. J. Glassbrenner, Phys. Rev. **120**, 782 (1960).
[14]C. J. Glassbrenner and G. A. Slack, Phys. Rev. **134**, A1058 (1964).
[15]J. E. Parrott, Phys. Status Solidi B **48**, K159 (1971).
[16]G. P. Srivastava, *The Physics of Phonons* (Adam Hilger, Bristol, 1990).
[17]M. Asen-Palmer, K. Bartkowski, E. Gmelin, M. Cardona, A. P. Zhemov, A. V. Inyushkin, A. Taldenkov, V. I. Ozhogin, K. M. Itoh, and E. E. Haller, Phys. Rev. B **56**, 9431 (1997).
[18]D. T. Morelli, J. P. Heremans, and G. A. Slack, Phys. Rev. B **66**, 195304 (2002).
[19]Y. Ezzahri and A. Shakouri, Phys. Rev. B **79**, 184303 (2009).
[20]Y. Ezzahri, K. Joulain, and A. Shakouri, J. Heat. Transfer. **133**, 072401 (2011).
[21]G. D. Mahan and F. Claro, Phys. Rev. B **38**, 1963 (1988).
[22]D. D. Joseph and L. Preziosi, Rev. Mod. Phys. **61**, 41 (1989).
[23]A. A. Joshi and A. Majumdar, J. Appl. Phys. **74**, 31 (1993).
[24]G. Chen, Phys. Rev. Lett. **86**, 2297 (2001).
[25]F. X. Alvarez and D. Jou, Appl. Phys. Lett. **90**, 083109 (2007).
[26]F. X. Alvarez and D. Jou, J. Appl. Phys. **103**, 094321 (2008).
[27]M. E. Siemensi, Q. Li, R. Yang, K. A. Nelson, E. H. Anderson, M. M. Murnane, and H. C. Kapteyn, Nature. **9**, 26 (2010).
[28]H. Iwai, Microelectron. Eng. **86**, 1520 (2009).

[29]R. A. Guyer and J. A. Krumhansl, Phys. Rev. **133**, A1411 (1964).
[30]R. A. Guyer and J. A. Krumhansl, Phys. Rev. **148**, 766 (1966).
[31]R. A. Guyer and J. A. Krumhansl, Phys. Rev. **148**, 778 (1966).
[32]S. G. Volz and G. Chen, Phys. Rev. B **61**, 2651 (2000).
[33]S. G. Volz, Phys. Rev. Lett. **87**, 074301 (2001).
[34]B. Hüttner, Phys. Status Solidi B **245**, 2786 (2008).
[35]B. S. Shastry, Phys. Rev. B **73**, 085117 (2006).
[36]B. S. Shastry, Rep. Prog. Phys. **72**, 016501 (2009).
[37]Y. K. Koh and D. G. Cahill, Phys. Rev. B **76**, 075207 (2007).
[38]D. G. Cahill, Rev. Sci. Instrum. **75**, 5119 (2004).
[39]A. J. Schmidt, X. Chen, and G. Chen, Rev. Sci. Instrum. **79**, 114902 (2008).
[40]S. Dilhaire, G. Pernot, G. Calbris, J. M. Rampnoux, and S. Grauby, J. Appl. Phys. **110**, 114314 (2011).
[41]N. W. Ashcroft and N. D. Mermin, *Solid State Physics*, 2nd ed. (Holt Rinehart and Winston, New York, 1976).
[42]R. O. Pohl, Phys. Rev. **118**, 1499 (1960).
[43]B. K. Agrawal and G. S. Verma, Phys. Rev. **128**, 603 (1962).
[44]M. E. Gurtin and A. C. Pipkin, Arch. Ration. Mech. Anal. **31**, 113 (1968).
[45]W. Hafez and M. Feng, Appl. Phys. Lett. **86**, 152101 (2005).
[46]M. Feng, N. Holonyak, Jr., G. Walter, and R. Chan, Appl. Phys. Lett. **87**, 131103 (2005).
[47]G. A. Slack and M. A. Hussain, J. Appl. Phys. **70**, 2694 (1991).
[48]See http://www.ioffe.ru/SVA/NSM/Semicond/index.html for a very interesting collection of experimental data on various physical properties of the main semiconductor crystals. All information is supported by a full list of references.
[49]N. Mingo, D. Hauser, N. P. Kobayashi, M. Plissonier, and A. Shakouri, Nano. Lett. **9**, 711 (2009).
[50]W. Kim, J. Zide, A. Gossard, D. Klenov, S. Stemmer, A. Shakouri, and A. Majumdar, Phys. Rev. Lett. **96**, 045901 (2006).
[51]A. J. Minnich, J. A. Johnson, A. J. Schmidt, K. Esfarjani, M. S. Dresselhaus, K. A. Nelson, and G. Chen, Phys. Rev. Lett. **107**, 095901 (2011).
[52]A. J. Minnich, G. Chen, S. Mansoor, and B. S. Yilbas, Phys. Rev. B **84**, 235207 (2011).
[53]K. Esfarjani, G. Chen, and H. T. Stokes, Phys. Rev. B **84**, 085204 (2011).